Int. J. Electrochem. Sci., 17 **(2022)** Article Number: 220944, doi: 10.20964/2022.09.79

International Journal of
ELECTROCHEMICAL
SCIENCE
www.electrochemsci.org

Modeling of Enzyme Adsorption and Surface Enzyme Reaction Kinetics in Biopolymer Microarrays

S. Salai Sivasundari[1], *B. Manimegalai*[1], *L. Rajendran*[1,*], *Michael EG Lyons*[2,*]

[1] Department of Mathematics, AMET University, Kanathur-603112, Chennai, India.
[2] School of Chemistry & AMBER National Centre, University of Dublin, Trinity College Dublin, Dublin 2, Ireland.
[*]E-mail: raj_sms@rediffmail.com, melyons@tcd.ie

Received: 9 June 2022 / *Accepted:* 10 July 2022 / *Published:* 7 August 2022

The surface enzymatic reactions on biopolymer microarrays incorporating enzyme adsorption and surface enzyme reaction are discussed. This model is based on one-dimensional first-order nonlinear equations with a nonlinear term related to Langmuir adsorption and Michaelis-Menten kinetics. This equation is solved analytically using the homotopy perturbation method for deriving the fractional surface coverages of three species at the reacted and unreacted surfaces. The normalized signal response consists of three rate constants (enzyme adsorption, enzyme de-sorption and enzyme catalysis), and a diffusion parameter is reported. The influence of the parameter on fractional surface coverage is also reported. The obtained analytical results are compared with simulation results for the experimental values of parameters, and satisfactory agreement is noted.

Keywords: Surface enzyme kinetics, Langmuir adsorption, Biopolymer microarrays, Non-linear equations, Homotopy perturbation method.

1. INTRODUCTION

The biopolymers attached to surfaces in a microarray format to analyze affinity interactions have become a crucial tool for modern biology, biochemistry, and biotechnology. Surface plasmon resonance imaging (SPRI) has recently emerged as a highly flexible method for detecting biopolymer (e.g., DNA, RNA, peptide, protein, carbohydrate) microarray adsorption [1]. SPRI can also detect the adsorption of many biomolecules, including DNA, RNA, lectins, and antibodies [2-7].

The surface enzymatic reaction rates have been studied quantitatively using various analytical methods. At the same time, most research approaches have been focused on the fluorescent based technique [8–10] and the SPR-based technique [11–14]. The kinetics of enzyme reactions and Langmuir adsorption on surfaces can be studied using the SPR technique. Takashi Kakiuchi and colleagues [15]

developed a kinetic model to describe how phospholipase D breaks down phosphatidylcholine monolayers. These models integrate the hydrolysis kinetic model at the interface and the enzyme diffusion from the bulk to the bulk interface.

A recent approach that links adsorption and enzyme kinetics has been proposed by Lee and coworkers [16] for analyzing enzyme-catalyzed surface reactions. Lee et al. [17] derived the fractional surface coverage using Euler integration methods. Manimozhi and Rajendran [18] derived an analytical expression of fractional surface coverages for the Langmuir kinetics model without catalytic activity.

The Authors are unaware of the analytical results for the fractional surface coverage of all species up to this date [16]. In this communication, the closed and simple analytical expression of surface coverage of all species is derived in the presence of catalytic activity. The surface enzyme kinetics for biopolymer microarrays are analysed using these analytical results. The maximum value of the surface coverages of intermediate species and the time to reach the maximum value in terms of rate constants are also reported. The derived analytical results were compared with simulation results for the experimental values of parameters, and good agreement was observed.

2. THEORY

Recently Lee et al. [17] developed SPRI and SPFS measurements to determine the rate constant in enzyme surface catalysis reactions. The three processes depicted in Figure 1 define the simplest possible model for the surface enzyme reaction. This reaction scheme can be written as follows:

$$E_{(x=\infty)} \xrightarrow{k_\infty} E_{(x=0)}, \quad S + E_{(x=0)} \underset{K_2}{\overset{K_1}{\rightleftharpoons}} ES, \quad ES \xrightarrow{k_{cat}} S^* + E_{(x=0)} \tag{1}$$

where $E_{(x=\infty)}$ and $E_{(x=0)}$ are the bulk and surface enzyme concentrations. S is the RNA-DNA surface bound substrate (the RNA-DNA heteroduplex), ES is the surface enzyme-substrate complex (the RNase H-heteroduplex complex), $S^*$is the surface product (ssDNA), and k_{cat} is the surface reaction rate for the enzyme complex. The steady-state mass transport coefficient (k_m), which is also known as D/δ, controls the diffusion in the case of SPRI in microfluidic channels, where D is the enzyme's diffusion coefficient and δ is the thickness of the steady-state diffusion layer.This condensed model also makes the assumption that there are only simple, non-interacting 1:1 substrate-enzyme surface complexes and that the enzyme E does not bind to inactive surface sites.

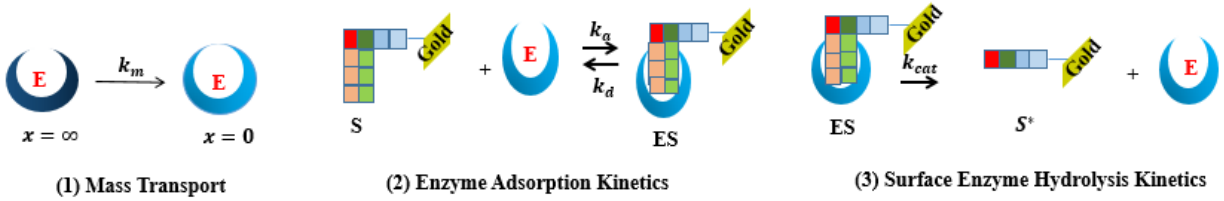

Figure 1. Reaction scheme of surface enzymatic process [16].

The kinetics for this reaction scheme are governed by the following nonlinear equations [16].

$$\theta_S(t) + \theta_{ES}(t) + \theta_{S^*}(t) = 1 \tag{2}$$

$$\frac{d\theta_{ES}(t)}{dt} = \frac{k_a[E]\left(1-\theta_{ES}(t)-\theta_{S^*}(t)\right)-(k_d+k_{cat})\theta_{ES}(t)}{1+\beta(1-\theta_{ES}(t)-\theta_{S^*}(t))} \tag{3}$$

$$\frac{d\theta_{S*}(t)}{dt} = k_{cat}\theta_{ES}(t) \quad (4)$$

The initial conditions are

$$\theta_S(t=0) = 1, \theta_{ES}(t=0) = 0 \text{ and } \theta_{S^*}(t=0) = 0 \quad (5)$$

where the fractional surface coverages for the three surface species S, ES, and S^* are denoted as

$$\theta_x(t) = \frac{\Gamma_x}{\Gamma_{tot}} \quad (6)$$

where $x = S, ES,$ or S^*, $[E]$ is the bulk enzyme concentration, and β is a dimensionless diffusion parameter defined by the following equation.

$$\beta = \frac{k_a\,\Gamma_{tot}}{k_m} = \frac{k_a\,\Gamma_{tot}\delta}{D} \quad (7)$$

This study uses the homotopy perturbation method to solve the nonlinear equations (2-4) [19–23]. The concept for this method was initially proposed by He [24]. The constraints of the conventional perturbation methods have been overcome by this method, which combines the classical perturbation and homotopy techniques. By using this technique, in this work the analytical expressions of fractional surface coverage for the three species are derived.

3. RESULTS AND DISCUSSION

The approximate analytical expression of fractional surface coverage for the three surface species S, ES, and S^* are obtained using HPM as follows (See supplementary material):

$$\theta_S(t) = 1 - \theta_{ES}(t) - \theta_{S^*}(t) \quad (8)$$

$$\theta_{ES}(t) \approx \frac{2k_a[E]}{\sqrt{a}}\, e^{\frac{-mt}{2(1+\beta)}} \left\{ sinh\left(\frac{\sqrt{a}\,t}{2(1+\beta)}\right)\right\} \quad (9)$$

$$\theta_{S*}(t) \approx 1 - e^{\frac{-mt}{2(1+\beta)}} \left[\frac{m}{\sqrt{a}}\, sinh\left(\frac{\sqrt{a}t}{2(1+\beta)}\right) + cosh\left(\frac{\sqrt{a}t}{2(1+\beta)}\right)\right] \quad (10)$$

The fractional surface coverage of ES on the unreacted surface using Eqs. (9-10) we get,

$$\lambda_{ES}(t) = \frac{\theta_{ES}(t)}{1-\theta_{S^*}(t)} \approx \frac{2k_a[E]}{m+\sqrt{a}\coth\left(\frac{\sqrt{a}t}{2(1+\beta)}\right)} \quad (11)$$

where, $a = m^2 - 4k_a[E]k_{cat}(1+\beta), m = k_a[E] + k_{cat} + k_d$ (12)

The analytical expression for the fractional surface coverage for the three surface species S, ES, and S^* is valid provided the parameter $a > 0$. Eqs. (8-10), represent the new analytical expressions for the surface coverage $\theta_S,\ \theta_{ES},\ \theta_{s*}$ for all values of rate constant $k_a[E],\ k_{cat}, k_d$ and diffusion parameter, β. The Eq. (11) is a closed analytical expression of fraction of unreacted surface sites, λ_{ES}.

3.1 Validation of analytical results

Lee et al. [16] obtained the time-dependent surface coverages $\theta_{ES}(t),\ \theta_S(t)$, and $\theta_{S^*}(t)$ profile over the course of the enzymatic reaction by solving the Eqs. (2-4) using numerical methods. Figs. 2(a-d) shows the profiles of relative surface coverage $\theta_S, \theta_{ES}, \theta_{s*}$ for various experimental values of parameters (Table. A1). Our analytical results are compared with simulation results (Maple-19 software) in Figs. 2(a-d). A satisfactory agreement is noted.

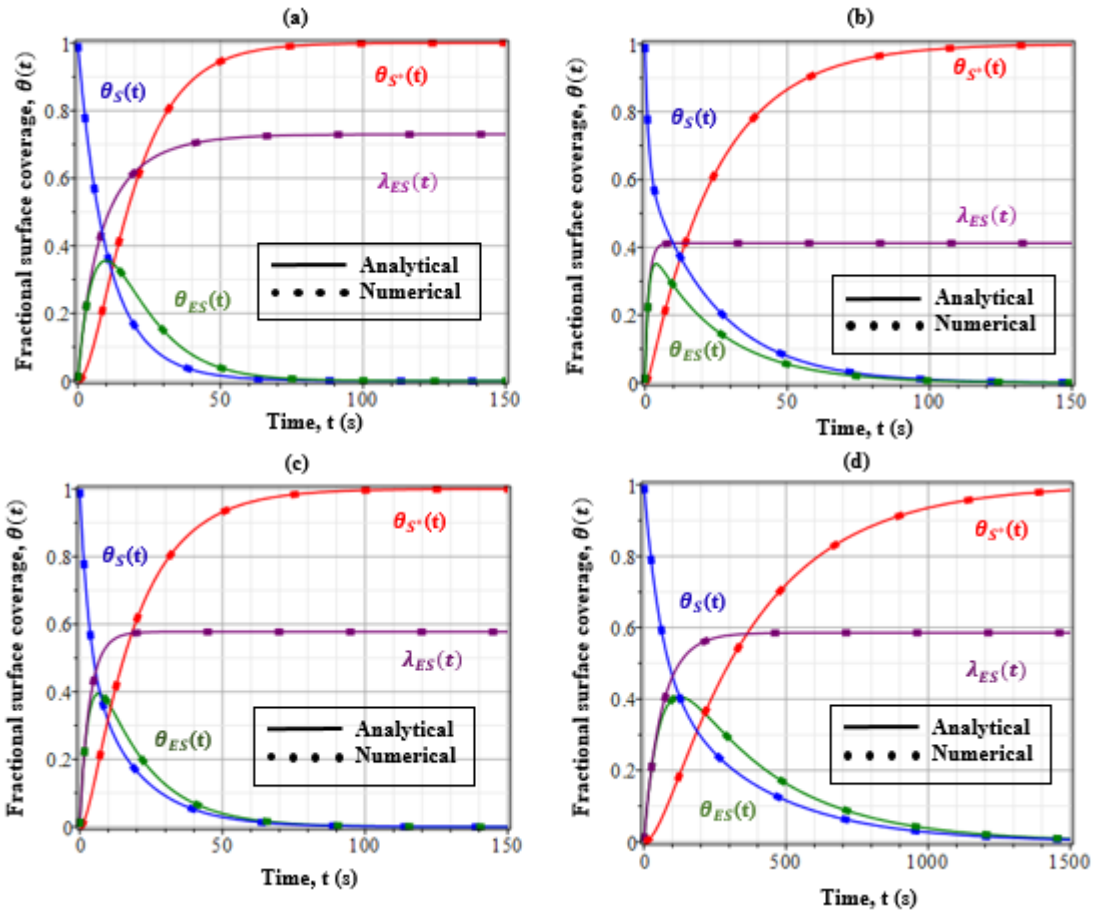

Figure 2. Comparison of analytical expression of fractional surface coverages $\theta_S, \theta_{ES}, \theta_{s*}$ and λ_{ES} (Eqs. (8-11)) with simulation results for various experimental values of parameters.

3.2 Characteristics of the fractional surface coverages

The characteristics of the fractional surface coverages $\theta_S, \theta_{ES}, \theta_{s*}$ and λ_{ES} which is observed from the analytical results (Eqs. (8-11)) are summarized in Table.1. These results are also confirmed in Fig. 2.

Table 1. Characteristics of the fractional surface coverage profiles

Relative surface coverage	Increasing/decreasing function	Minimum value	Maximum value
$\theta_S(t)$	Decreasing function	$\theta_{S_{min}} = 0$ (at $t = \infty$)	$\theta_{S_{max}} = 1$ (at $t = 0$)
$\theta_{ES}(t)$	Pulsatile function	$\theta_{ES_{min}} = 0$ (at $t = 0$ and $t = \infty$)	$\theta_{ES_{max}} = \frac{2k_a[E]}{m+\sqrt{a}}\left(\frac{m-\sqrt{a}}{m+\sqrt{a}}\right)^{\frac{1}{2}\left(\frac{m}{\sqrt{a}}-1\right)}$ $t_{max} = \frac{1+\beta}{\sqrt{a}}\ln\left(\frac{m+\sqrt{a}}{m-\sqrt{a}}\right)$
$\theta_{s*}(t)$	Increasing function	$\theta_{s^*min} = 0$ (at $t = 0$)	$\theta_{s^*max} = 1$ (at $t = \infty$)
$\lambda_{ES}(t)$	Increasing function	$\lambda_{ES_{min}} = 0$ (at $t = 0$)	$\lambda_{ES_{max}} = \frac{2k_a[E]}{m+\sqrt{a}}$ (at $t = \infty$)

In addition, from these figures, it is inferred that the surface coverage $\theta_{ES}(t)$ increases abruptly and attains the maximum at the time t_{max} and then decreases slowly and reaches its steady-state value. This result is also confirmed in Fig. 2(b) for the value of parameters,$k_a[E] = 2\ s^{-1}$, $k_{cat} = 0.1\ s^{-1}, k_d = 3\ s^{-1}, \beta = 5$. The maximum value is 0.3513 at $t = 3.8781\ s$.

Fractional surface coverages $\theta_S, \theta_{ES}, \theta_{S*}$ and λ_{ES} from Eqs. (8-11) can be obtained as follows for short time:

$$\theta_S(t) = 1 - \frac{k_a[E]t}{(1+\beta)} + \frac{mt^2}{2(1+\beta)^2}\left(k_a[E] - \frac{m}{2}\right) \quad (13)$$

$$\theta_{ES}(t) \approx \frac{k_a[E]t}{(1+\beta)}\left(1 - \frac{mt}{2(1+\beta)}\right) \quad (14)$$

$$\theta_{S*}(t) \approx \left(\frac{mt}{2(1+\beta)}\right)^2 \quad (15)$$

$$\lambda_{ES}(t) \approx \frac{2k_a[E]\,t}{mt+2(1+\beta)} \quad (16)$$

The steady-state $(t \to \infty)$ fractional surface coverage of the species can also be calculated using Eq. (8-11) as follows:

$$\theta_S(t \to \infty) = \theta_{ES}(t \to \infty) = 0, \theta_{S*}(t \to \infty) = 1, \lambda_{ES}(t \to \infty) = \frac{2k_a[E]}{m+\sqrt{a}} \quad (17)$$

3.3. Effect of the parameters on the steady-state fractional surface coverage (λ_{ES}).

The analytical expression of steady-state value of λ_{ES} from the Eq. (11) can be written as follows:

$$\lambda_{ES} = \frac{2k_a[E]}{k_a[E]+k_{cat}+k_d+\sqrt{(k_a[E]+k_{cat}+k_d)^2-4k_a[E]k_{cat}(1+\beta)}} \quad (18)$$

The steady-state value of λ_{ES} depends on the relative values of k_{cat}, $k_a[E]$, β and k_d.

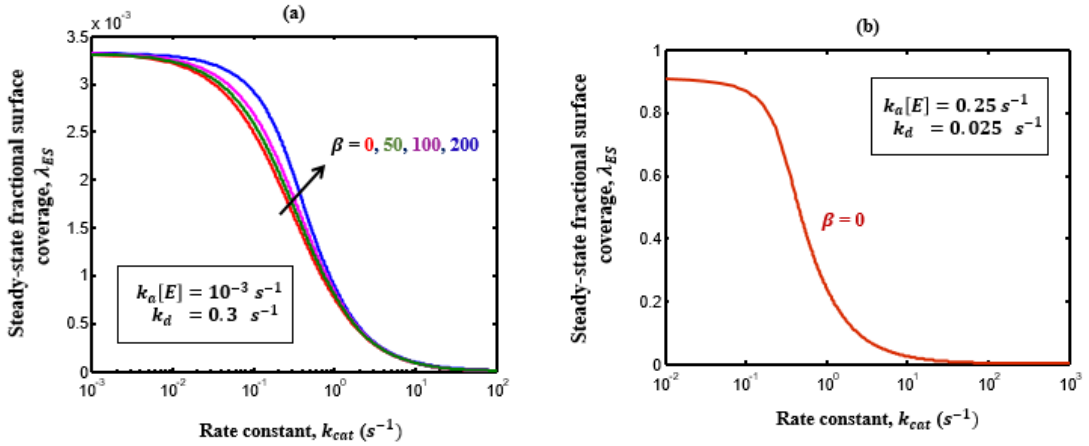

Figure 3. Deviation of steady-state fractional surface coverage (λ_{ES}) versus k_{cat} (s^{-1}) using Eq.(11).

Figure 3(a-b) plots the variation of λ_{ES} as a function of k_{cat} with some fixed values of other parameters. From Fig. 3a, it is inferred that λ_{ES} increases when diffusion parameter increases. From the figure it is also observed that there is significant difference of λ_{ES} with respect to the diffusion parameter β. In addition, the parameter $k_a[E]$ produce the more effect on fractional surfaces. This is also confirmed in Fig.5. Table 2 lists the steady-state value of λ_{ES} for extreme enzyme adsorption,

desorption, catalysis rate constant, and diffusion parameter values. The enzyme adsorption kinetics will only constrain the velocity of the surface enzyme reaction if k_{cat} is significantly greater than $k_a[E]$. In this instance, $\lambda_{ES} = 0$.

Table 2. Characteristic of the steady-state value of λ_{ES} for extreme values of rate constant.

Value of diffusion parameter / Rate constant	**Steady-state fractional surface coverage λ_{ES}**
$\beta = 0$ (Diffusion parameter)	$\lambda_{ES} = 2k_a[E]\left[k_a[E] + k_{cat} + k_d + \sqrt{(k_a[E] + k_{cat} + k_d)^2 - 4k_a[E]k_{cat}}\right]^{-1}$
$k_{cat} = 0$ (Catalytic rate constant)	$\lambda_{ES} = \frac{k_a[E]}{k_a[E] + k_d}$
$k_{cat} \to \infty$ or $k_d \to \infty$ or $k_a[E] = 0$ (Catalytic and desorption rate constant) or (Kinetic enzyme parameter)	$\lambda_{ES} = 0$
$k_a[E] \to \infty$ (Kinetic enzyme parameter)	$\lambda_{ES} = 2$
$k_{cat} = k_a[E]$	$\lambda_{ES} = 2k_a[E]\left[2k_a[E] + k_d + \sqrt{k_d(4k_a[E] + k_d) - 4\beta(k_a[E])^2}\right]^{-1}$
$k_{cat} \gg k_a[E]$	$\lambda_{ES} = \frac{k_a[E]}{k_{cat} + k_d} \approx 0$

3.4 Normalized signal response

The normalized signal response is the difference of two components .The normalized signal, which responds to both enzyme adsorption, and surface loss is obtained as follows:

$$\Delta\%R(t) = \theta_{ES}\,(t) - \theta_{S^*}(t) \approx \frac{e^{\frac{-mt}{2(1+\beta)}}}{\sqrt{a}}\left[(m + 2k_a[E])\sinh\left(\frac{\sqrt{a}t}{2(1+\beta)}\right) + \sqrt{a}\cosh\left(\frac{\sqrt{a}t}{2(1+\beta)}\right)\right] - 1 \tag{19}$$

where, m and a are the parameters defined in Eq. (12).

Figure 4 compares theoretical curves with experimental results for the normalized signal response for enzyme concentrations ranging from 50 *nM* to 320 *nM*. From the figure, it is observed that an increase in enzyme concentration leads to an increase in the peak value of the normalized signal response. This figure also shows that the pulsatile normalized signal response initially increases rapidly due to enzyme adsorption and reaches the maximum value, and then gradually decreases due to heteroduplex hydrolysis and release of enzyme back into solution to a steady-state value.

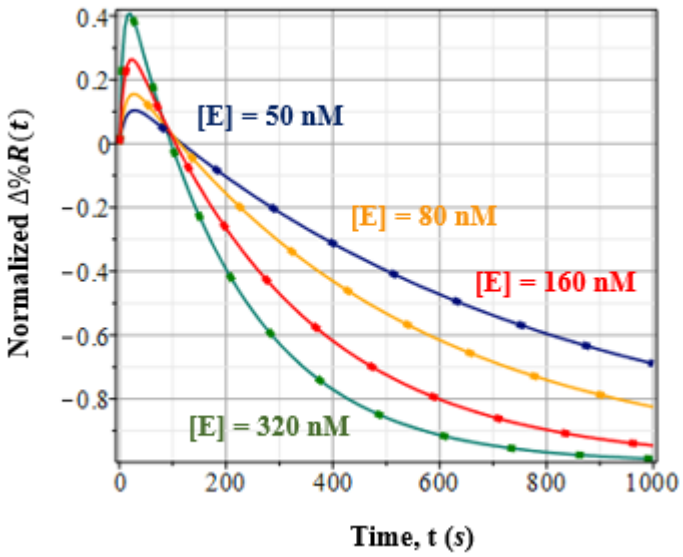

Figure 4. The plot of normalized signal response Δ%R versus time t (s) for experimental values of parameters [16] for different values of enzyme concentrations $[E]$ (nM). The dotted line represent the analytical result and solid line represent the experimental result.

3.5 Differential sensitive analysis of parameters

Eq. (13) gives a new approximate analytical expression for the non-steady-state fractional surface coverage of the species ES on the unreacted surface for all values of parameter. The impact of these parameters on the fractional surface coverage λ_{ES} can be determined by partially differentiating the fractional surface coverage with respect to these parameters.

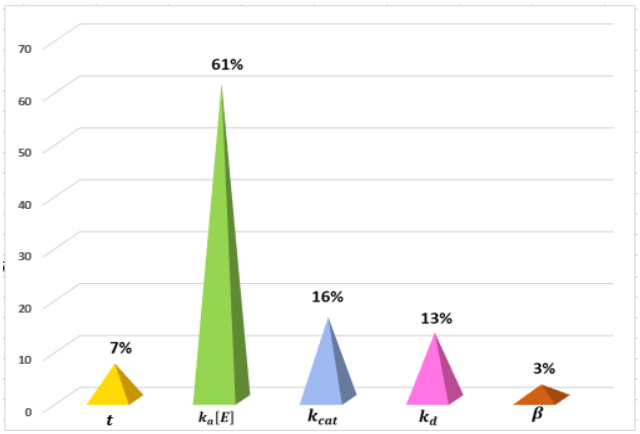

Figure 5. Sensitivity analysis of the parameters: Percentage change in fractional surface coverage for the surface species ES, at the unreacted surface (Eq.13) where $t = 5\ s, k_a[E] = 1\ s^{-1}, k_d = 2\ s^{-1}, k_{cat} = 0.1\ s^{-1}, \beta = 10$.

Figure 5 depicts the spreadsheet analysis of these results. With respect to $k_a[E], k_{cat}, k_d, t$ and β, the percentages of change in λ_{ES} are 61%, 16%, 13%, 7%, and 3%, respectively. As a result, it is clear that parameter $k_a[E]$ has a greater impact on λ_{ES}. This parameter is extremely sensitive. As a result, the adsorption rate constant (k_a) and enzyme concentration $([E])$ have a greater impact on the fractional

surface coverage of species on the unreacted surface than the other factors. The factors k_{cat} and k_d are referred to as moderately sensitive parameters because they influence λ_{ES} by 16% and 13%, respectively. The other two factors, time (t) and diffusion parameter (β), are less sensitive.

The model of enzyme adsorption and surface enzyme reaction kinetics was solved previously using the Euler integration method by Corn et al. [16]. He obtained the surface coverage profiles for all experimental values of parameters using the Euler integration method. In addition, Rajendran et al. [18] derived the approximate analytical solution for the fractional surface coverage profiles in the absence of diffusion parameter ($\beta = 0$). In this work, the effect of the parameters is found by using the analytical result.

Our approximate analytic/symbolic solutions for enzyme adsorption and surface enzyme reaction kinetics give the answers to a whole set of parameters. Also, our analytic approach gives a closed-form solution in terms of convergent series with easily computable components. But for every set of parameters, the numerical approach has to be recalculated. Analytical approaches can provide profound understanding, whereas general numerical approaches typically cannot. Numerical solutions can rarely contribute to proof of new ideas (finding the maximum or minimum, influence of parameters etc.). The strength of analytical solutions is typically regarded as significant. Therefore, developing new techniques for analytical solutions to nonlinear equations in surface enzyme kinetics for biopolymer is constantly of significant interest.

4. CONCLUSIONS

Theoretical investigations are made on the surface enzyme chemistry and bioaffinity interactions on biopolymer microarrays. In the absence of catalytic activity, the analytical expression of the surface coverage for the three surface species $S, ES,$ and S^* is obtained in terms of four fundamental parameters ($k_a[E], k_{cat}, k_d$ and β).The maximum fractional surface coverage, θ_{ES} and time to reach this peak value also reported. Fractional surface coverage of unreacted sites (λ_{ES}) and normalized signal response are discussed. The Maple-19 software is also used to present the numerical solution of this problem. The numerical results (or Euler integration method) are compared to our analytical results. Thus, a good agreement with the present simulation results is notified. Increases in the diffusion parameter increase the steady-state diffusion layer thickness. The kinetic enzyme parameter $k_a[E]$ has more influence on surface coverage profiles. The theoretical model described here can only apply to systems where the enzyme binds to a surface target in a 1:1 relationship with no mass transport constraints. This analytical method can be extended for modeling of complex biochemical system involving multiple binding of metal or charged ligands.

NOMENCLATURE:

Parameter	**Meaning**	**Units**
D	Diffusion coefficient	$cm^2\ s^{-1}$

$E_{(x=\infty)}$	Enzyme concentration in the bulk solution	nM
$E_{(x=0)}$	Enzyme concentration in the surface	nM
[E]	Enzyme concentration	nM
k_a	Enzyme adsorption rate constant	$M^{-1}s^{-1}$
k_d	Enzyme desorption rate constant	s^{-1}
k_{cat}	Enzyme catalysis rate constant	s^{-1}
$k_a[E]$	Kinetic enzyme parameter	s^{-1}
k_m	Mass transfer coefficient	s^{-1}
a	Parameter defined in Eq.(15)	s^{-2}
m	Parameter defined in Eq. (15)	s^{-1}
δ	Steady-state diffusion layer thickness	cm^2
Γ_x	Surface coverage	M
t	Time	s
Γ_{tot}	Total number of surface sites	M
β	Dimensionless diffusion parameter	None
θ_{ES}	Fractional surface coverages of the species ES on the reacted surface	None
θ_S	Fractional surface coverages of the species S on the reacted surface	None
θ_{S^*}	Fractional surface coverages of the species S^* on the reacted surface	None
λ_{ES}	Fractional surface coverages of ES on the unreacted surface	None
Δ%R	Normalized signal response	None

DECLARATION OF COMPETING INTEREST

The authors declare that they have no known competing financial interests or personal relationships that could have appeared to influence the work reported in this paper.

ACKNOWLEDGEMENT

The authors thank the reviewers for their insightful comments, which helped to improve the manuscript's quality**.** The authors express their gratitude to Shri J. Ramachandran, Chancellor, Col. Dr. G. Thiruvasagam, Vice-Chancellor and Dr. M. Jayaprakashvel, Registrar, Academy of Maritime Education and Training (AMET), Deemed university, Chennai, Tamil Nadu for their continuous encouragement.

Appendix A.

Table A1. Numerical value of kinetic parameter used in [17] and in this work.

Parameter	Name	Unit	Numerical value [17]	This work						
				Fig. 2				Fig. 3		Fig. 4
				(a)	(b)	(c)	(d)	(a)	(b)	
k_a	Adsorption rate constant	$M^{-1}s^{-1}$	2×10^5 to 3×10^6	-	-	-	-	-	-	2.2×10^5
[E]	Enzyme concentrations	nM	1 to 320	-	-	-	-	-	-	50, 80, 160, 320
$k_a[E]$	Kinetic enzyme parameter	s^{-1}	0.2×10^{-3} to 960×10^{-3}	0.1	2	2	5	10^{-3}	0.25	-
k_d	Desorption rate constant	s^{-1}	0.056 to 0.1	0.01	3	2	5	0.3	0.025	0.056
k_{cat}	Catalysis rate constant	s^{-1}	0.009 to 1	0.1	0.1	0.1	0.005	-	-	0.009
β	Dimensionless diffusion parameter	none	0 to 650	0	5	10	500	0, 50, 100,200	0	0

Appendix B

1. Analytical solutions of nonlinear Eq. (2) and Eq. (3) using HPM

The HPM constructed for Eq. (2) is as follows:

$$(1-p)\left((1+\beta)\frac{d\theta_{ES}}{dt} - k_a[E](1-\theta_{S^*}) + (k_a[E]+k_d+k_{cat})\theta_{ES}\right)$$

$$+p\left(\left(1+\beta(1-\theta_{ES}-\theta_{S^*})\right)\frac{d\theta_{ES}}{dt} - k_a[E](1-\theta_s^*) + (k_a[E]+k_d+k_{cat})\theta_{ES}\right) = 0 \qquad \text{(B1)}$$

The solution for the Eqs. (2-3) are

$$\theta_{ES}(t) = \theta_{ES_0}(t) + p\theta_{ES_1}(t) + \cdots \qquad \text{(B2)}$$

$$\theta_{S^*}(t) = \theta_{S^*_0}(t) + p\theta_{S^*_1}(t) + \cdots \qquad \text{(B3)}$$

Substituting and equating the coefficients of p^0, p^1 gives the following equations.

$$p^0\colon\ (1+\beta)\frac{d\theta_{ES_0}(t)}{dt} - k_a[E]\left(1-\theta_{S^*_0}(t)\right) + m\,\theta_{ES_0}(t) = 0 \qquad \text{(B4)}$$

$$p^0\colon\ \frac{d\theta_{S^*_0}(t)}{dt} = k_{cat}\theta_{ES_0}(t) \qquad \text{(B5)}$$

For solving Eq. (B4) and Eq. (B5), differentiate the Eq. (B4) with respect to t gives,

$$(1+\beta)\frac{d^2\theta_{ES_0}(t)}{dt^2} + k_a[E]\frac{d\theta^*_{S_0}(t)}{dt} + m\frac{d\theta_{ES_0}(t)}{dt} = 0 \qquad \text{(B6)}$$

From Eq. (B5), Eq. (B6) becomes,

$$(1+\beta)\frac{d^2\theta_{ES_0}(t)}{dt^2} + m\frac{d\theta_{ES_0}(t)}{dt} + k_a[E]k_{cat}\theta_{ES_0}(t) = 0 \quad \text{(B7)}$$

The respective boundary conditions are as follows:

$$\theta_{ES_0}(t=0) = 0 \quad \text{(B8)}$$

$$\frac{d\theta_{ES_0}}{dt}\ (t=0) = \frac{k_a[E]}{1+\beta} \quad \text{(B9)}$$

The above boundary condition (B9) is obtained from the Eq. (B4).

On solving the Eq. (B7) gives,

$$\theta_{ES_0}(t) = \frac{2k_a[E]}{\sqrt{a}}\ e^{-mt/2(1+\beta)}\left\{sinh\left(\frac{\sqrt{a}\,t}{2(1+\beta)}\right)\right\} \quad \text{(B10)}$$

Using the above equation, Eq. (B5) gives,

$$\theta_{S^*{}_0}(t) = 1 - e^{\frac{-mt}{2(1+\beta)}}\left[\frac{m}{\sqrt{a}}\ sinh\left(\frac{\sqrt{a}t}{2(1+\beta)}\right) + cosh\left(\frac{\sqrt{a}t}{2(1+\beta)}\right)\right] \quad \text{(B11)}$$

where,

$$a = m^2 - 4k_a[E]k_{cat}(1+\beta),\ m = k_a[E] + k_{cat} + k_d \quad \text{(B12)}$$

Using the first iteration, the solution of Eq. (3) and Eq. (4) is as follows:

$$\theta_{ES}(t) \approx \theta_{ES_0}(t) \quad \text{(B13)}$$

$$\theta_S^*(t) \approx \theta_{S^*{}_0}(t) \quad \text{(B14)}$$

We can find the next iteration to improve the accuracy of the results.

2. Maple code to find the analytical solution of nonlinear equations (2) to (6)

```
restart;with(DEtools);
kae := 2;kd := 2;kcat := 0.1;beta := 100;
DE1 := diff(u(t), t) - (kae*(1 - u(t) - v(t)) - (kd + kcat)*u(t))/(1 + beta*(1 - u(t) - v(t))) = 0, diff(v(t), t) -
kcat*u(t) = 0, w(t) + u(t) + v(t) = 1;
BC := u(0) = 0, v(0) = 0, w(0) = 1;
soln := dsolve({BC, DE1}, numeric);
y (t):= u(t)/(1 - v(t));
R(t) :=u(t) - v(t);
num1 := plots:-odeplot(soln, [t, y(t)], 0 .. 150, color = blue):
with(plots):
display(num1);
```

References

1. L.K. Wolf, D.E. Fullenkamp and R.M. Georgiadis, *J. Am. Chem. Soc.,* 127 (2005) 17453-17459.
2. V. Kanda, P. Kitov, D.R. Bundle and M.T. Mcdermott, *Anal. Chem.,* 77 (2005) 7497-7504.

3. M. Kyo, K. Usui Aoki and H. Koga, *Anal. Chem.,* 77 (2005) 7115-7121.
4. J.S. Shumaker Parry and C.T. Campbell, *Anal. Chem.* 76 (2004) 907-917.
5. E.A. Smith, W.D. Thomas, L.L. Kiessling, R.M. Corn, *J. Am. Chem. Soc.,* 125 (2003) 6140-6148.
6. G.J. Wegner, H.J. Lee and R.M. Corn, *Anal. Chem.,* 74 (2002) 5161-5168.
7. E.A. Smith, M. Kyo, H. Kumasawa, K. Nakatani, I. Saito and R.M. Corn, *J. Am. Chem Soc.,* 124 (2002) 6810-6811.
8. P.B. Gaspers, A.P. Gast and C.R. Robertson, *J. Colloid. Interface. Sci.,* 172 (1995) 518-529.
9. Y. Tachi-Iri, M. Ishikawa and K. Hirano, *Anal. Chem.,* 72 (2000) 1649-1656.
10. K. Tawa, W. Knoll, Nucl. *Acids. Res.,* 32 (2004) 2372-2377.
11. A.W. Peterson, L.K. Wolf and A.M. Georgiadis, *J. Am. Chem. Soc.,* 124 (2002) 14601-14607.
12. T.T. Goodrich, H.J. Lee and R.M. Corn, *J. Am. Chem. Soc.,* 126 (2004) 4086-4087.
13. G.J. Wegner, A.W. Wark, H.J. Lee, E. Codner, T. Saeki, S. Fang and R.M. Corn, *Anal. Chem.,* 76 (2004) 5677-5684
14. V. Kanda, J.K. Kariuki, D.J. Harrison and M.T. Mcdermott, *Anal. Chem.,* 76 (2004) 7257-7262.
15. T. Kondo, T. Kakiuchi and M. Senda, *Anal. Sci.,* 7 (1991) 1725.
16. H.J. Lee, A.W. Wark, T.T. Goodrich, S. Fang and R.M. Corn, *Langmuir*, 21 (2005) 4050-4057.
17. H.J. Lee, A.W. Wark and R.M. Corn, *Langmuir,* 22 (2006) 5241-5250.
18. P. Manimozhi and L. Rajendran, *J. Electroanal. Chem.,* 647 (2010) 87-92.
19. J.H. He and Y.O. El-Dib, *J. Math. Chem.,* 59 (2021) 1139-1150.
20. J.H. He and Y.O. El-Dib, J. Math. Chem., 58 (2020) 2245-2253.
21. B. Manimegalai, M.E.G. Lyons and L. Rajendran, *J. Electroanal. Chem.,* 902 (2021) 115775.
22. B. Manimegalai, L. Rajendran and M.E.G. Lyons, *Int. J. Electrochem. Sci.,* 16 (2021) 210946.
23. R. Joy Salomi, S. Vinolyn Sylvia, L. Rajendran and M.E.G. Lyons, *J. Electroanal. Chem.,* 895 (2021) 115421.
24. J.H. He, *Comput. Methods. Appl. Mech. Eng.,* 178 (1999) 257-262.